(1985-1986).

7. S. Srinivasan and C. Maggiore, in LANL Progress Report LA-9726-PR (May 1983).
8. B. C. Beard and P. N. Ross, LBL Report no. 21184 (March 1986).
9. P. N. Ross, EPRI Report EM-1553, Project 1200-5 (September 1980).
10. B. C. Beard, D. Dahlgren, and P. N. Ross, *J. Vac. Sci. Technol. A,* **3,** 2041 (1985).
11. W.-K. Chu, J. W. Mayer, and M.-A. Nicolet, "Backscattering Spectrometry," Academic Press, Inc., New York (1978).
12. H. Angerstein-Kozlowska, in "Comprehensive Treatise of Electrochemistry," Vol. 9, E. Yeager, J. O'M. Bockris, B. E. Conway, and S. Sarangapani, Editors, p. 15, Plenum Press, New York (1981).
13. J. Giner, *This Journal,* **111,** 376 (1964).
14. R. Woods, in "Electroanalytical Chemistry," Vol. 9, A. J. Bard, Editor, p. 1, Marcel Dekker, Inc., New York (1976).
15. P. R. Bevington, "Data Reduction and Error Analysis for the Physical Sciences," p. 56, McGraw-Hill, Inc., New York.
16. H. Angerstein-Kozlowska, B. E. Conway, and W. B. A. Sharp, *J. Electroanal. Chem. Interfacial Electrochem.,* **43,** 9 (1973).
17. S. Gottesfeld, M. T. Paffett, and A. Redondo, *ibid.,* **205,** 163 (1986).

18. L. R. Doolittle, *Nucl. Instr. Methods, B,* **9,** 344 (1985).
19. D. Jahn and W. Vielstich, *This Journal,* **109,** 849 (1962).
20. J. T. Glass, G. L. Cahen, Jr., G. E. Stoner, and E. J. Taylor, *This Journal,* **134,** 58 (1987).
21. M. R. Tarasevich, A. Sadkowski, and E. Yeager, in "Comprehensive Treatise of Electrochemistry," Vol. 7, B. E. Conway, J. O'M. Bockris, E. Yeager, U. M. Khan, and R. E. White, Editors, p. 301, Plenum Press, New York (1983).
22. F. T. Wagner and P. N. Ross, *Appl. Surf. Sci.,* **24,** 87 (1985).
23. G. Bouyssoux, M. Romand, H. D. Polaschegg, and J. T. Calow, *J. Electron Spectrosc. Relat. Phenom.,* **11,** 185 (1977).
24. M. Seo, R. Saito, and N. Sato, *This Journal,* **127,** 1909 (1980).
25. P. Stonehart, NASA Report NASA-CR-168223 (June 1984).
26. M. Weber, M. J. Dignam, S.-M. Park, and R. D. Venter, *This Journal,* **133,** 734 (1986).
27. H. R. Kunz, in "The Electrocatalysis of Fuel Cell Reactions," W. E. O'Grady, S. Srinivasan, and R. F. Dudley, Editors, p. 14, The Electrochemical Society Softbound Proceedings Series, Princeton, NJ (1978).
28. P. N. Ross, Jr., in "Electrocatalysis," W. E. O'Grady, P. N. Ross, Jr., and F. G. Will, Editors, p. 24, The Electrochemical Society Softbound Proceedings Series, Pennington, NJ (1982).

Synthesis and Photoelectrochemistry of Polycrystalline Thin Films of p-WSe$_2$, p-WS$_2$, and p-MoSe$_2$

Carlos R. Cabrera** and Hector D. Abruña*

Department of Chemistry, Baker Laboratory, Cornell University, Ithaca, New York 14853

ABSTRACT

Polycrystalline thin films (PTF) of p-WSe$_2$, p-WS$_2$, and p-MoSe$_2$ have been prepared and characterized with respect to their photoelectrochemical properties. p-WS$_2$ showed the highest open-circuit photovoltages and the highest conversion efficiencies in various redox couples. In addition, the band structure of all the films has been determined experimentally and compared to those reported for single crystals.

Over the last two decades a great deal of interest has developed in the area of photoelectrochemistry, particularly in the application of photoelectrochemical systems to the problem of solar energy conversion and storage. The interest is to develop new energy sources to supplement and eventually replace fossil fuels.

The first photoelectrochemical experiment was performed in 1839 by Becquerel (1), who demonstrated that a voltage and current are generated when a silver chloride electrode, immersed in an electrolytic solution and connected to a counterelectrode, is illuminated. Although the concept of a semiconductor did not exist at that time, it is now clear that the electrode which Becquerel used had semiconducting properties. In 1955, Brattain and Garett (2) used germanium as the first semiconductor electrode in photoelectrochemistry. Since then, the knowledge of semiconductors has grown steadily. Fujishima and Honda (3) were the first to point out the potential application of photoelectrochemical systems for solar energy conversion and storage. They demonstrated that the photo-oxidation of water to O$_2$ was possible by utilizing an n-type semiconducting titanium dioxide photoanode. Since then, there has been a large and rapidly growing international interest in the study of photoelectrochemistry of semiconductors (4).

The effective use of solar energy in photovoltaic or photoelectrochemical applications depends in part on the development of materials that can show high conversion efficiencies and long-term stability under operation. In ad-

dition, the desirable materials should have a bandgap that closely matches the solar spectrum and be made of readily available and inexpensive materials.

We have focused our attention on the transition metal dichalcogenides (*e.g.,* WSe$_2$, WS$_2$, MoSe$_2$, and others), also known as layered or d-d semiconductors. Tributsch's (5, 6) pioneering work on the use of these materials has stimulated intensive research in this area, and single crystals of a number of materials have been studied extensively in both aqueous and nonaqueous solvents and in photovoltaic and photoelectrosynthetic cells. The advantages of using these materials are that they have bandgaps (1.1-1.6 eV) that closely match the solar spectrum and exhibit high conversion efficiencies as single crystals. In addition, they can achieve long-term stability due to the fact that the transitions are localized in the nonbonding d orbitals of the metal. These materials consist of metal dichalcogenide sandwiches (*e.g.,* Se-W-Se) held together by van der Waals forces. The fact that there is strong covalent bonding within the layers, but only weak interactions between layers, makes these materials highly anisotropic in their properties. For example, the surface parallel to the C axis ($\parallel$C) is more conducting than the surface perpendicular to the C axis ($\perp$C). Therefore, edges and surface imperfections on the surface parallel to the C axis act as efficient recombination centers for photogenerated carriers or products (7, 8). As a result, the observed efficiencies are strongly dependent on the nature of the surface of the individual crystals. Although single crystals of these materials have shown very high efficiencies (9), they are typically of small area (due to the difficulty of growing large area single crystals

(10), making their use for large-scale conversion of solar energy impractical.

Polycrystalline thin films, on the other hand, can be grown as large area thin films with simple experimental procedures. Lewerenz and co-workers (11) had mentioned the possibility of using polycrystalline layers of transition metal dichalcogenide semiconductors. However, one must remember that because a polycrystalline film is expected to have a very high density of surface imperfections and exposed edges, one would *a priori* expect very little, if any, photoeffect on these materials due to the expected severe recombinational losses. However, these can be diminished with surface modification since it has been demonstrated that such treatments can enhance the rates of interfacial charge transfer (12), and achieve catalytic effects, as well as decrease recombinational losses (13).

Since the first work by Tributsh, extensive research has been done on single crystals of transition metal dichalcogenides. Selected single crystals of WSe$_2$ (9b), WS$_2$ (14), and MoSe$_2$ (15), have shown efficiencies of 10.2, 6, and 9.4%, respectively. On the other hand, reports on the use of polycrystalline materials have been somewhat limited. Cahen and co-workers (16a) prepared polycrystalline MoS$_2$ electrodes in a variety of ways, including covering a titanium substrate with the polycrystalline material, pressing pellets and binding within a polymer matrix. In general, only modest photoeffects were obtained with these. Ginley, Parkinson, and co-workers (16b) prepared polycrystalline n-WSe$_2$ electrodes by hot pressing microcrystalline powder. They also employed a variety of surface treatments in an effort to minimize recombinational losses. Schneemeyer and Cohen (16c) prepared polycrystalline n-MoS$_2$ by electrochemical growth from the melt at 800°C. Again, only modest photoresponses were obtained. Most recently, Di Paola (16d) reported on the preparation of polycrystalline p-WS$_2$ electrodes by reaction of H$_2$S with metallic tungsten or tungsten oxide films.

We have already demonstrated a way to synthesize PTF of p-WSe$_2$ and enhance the properties and efficiencies of these films by surface modification with o-phenylene diamine (OPD) (17). We also showed that surface modification with polybenzylviologen and colloidal platinum and [Re(CO)$_3$(v-bpy)Cl] rendered the PTF of p-WSe$_2$ active in the photoassisted evolution of H$_2$ (17) and the photoelectrocatalytic reduction of CO$_2$, respectively (18).

We now report on the preparation and photoelectrochemical characterization of polycrystalline thin films of p-WS$_2$ and p-MoSe$_2$ and compare them to the PTF of p-WSe$_2$. We compare photocurrent spectra, cyclic voltammetry, and efficiencies in photovoltaic cells. In addition, the band structure for each of the materials (bandgap, valence band, conduction band, and flatband potential) was determined experimentally and compared to reported values.

Experimental

(a) Synthesis of polycrystalline thin films (PTF) of transition metal dichalcogenides.—The synthesis of the polycrystalline thin films was performed in a quartz ampul (15 cm long and 2 cm diam) which had been previously cleaned with 48% HF, 1:1 HNO$_3$/HCl, and 48% HF with thoroughly rinsing with water after each cleaning. The ampul was oven dried. 10g of the desired transition metal dichalcogenide [WSe$_2$ (99.95%), WS$_2$ (99.8%), or MoSe$_2$ (99.9%); Atomergic Chemetals Corp. or Gallard-Schlesinger Chemical Mfg. Corp.] were placed inside the ampul, which was subsequently evacuated for at least 1h to a residual pressure of *ca.* 5 × 10^{-5} torr. At that time, the ampul

was sealed under vacuum and placed in a muffle furnace (Thermolyne Model 2000) whose temperature was raised slowly (*ca.* 100°C per hour) up to the desired temperature and was left for a prescribed amount of time for film growth. Table I presents the details of the growth temperatures and times. After film growth, the furnace was turned off and allowed to reach room temperature. Some of the powder is transported from the bottom of the ampul and deposited on the ampul walls. Two surfaces or sides can be defined; a shiny side (smooth side) which was that side in contact with the quartz ampul and a black matte side (rough side) which was that facing the ampul during the film growth. The ampul was opened and the material that had deposited on the walls was used as electrodes. The films could be mounted as electrodes right on the broken pieces of the quartz, or free standing films could be employed when they could be dislodged from the quartz. The electrodes were connected to a copper wire lead with silver paint (Acme Industries, New Haven, CT) on the front or back surface for films on quartz or free standing films, respectively. However, when performing experiments with the smooth side as the photoactive side, only free standing films could be used. In this case, the contact was done on the rough surface side. The wire was inserted into a piece of 6 mm glass tubing and the electrodes were masked with either 5 min epoxy, Torr-Seal (Varian Associates, Palo Alto, CA), or Chemgrip Cement (Chemplast Inc., Wayne, NJ) except for the surface to be studied. Typical electrode areas were about 0.1-0.2 cm^2.

(b) Instrumentation.—Electrochemical experiments were performed using a Princeton Applied Research Model 173 Potentiostat/Galvanostat in conjunction with a Model 179 Digital Coulometer and Model 175 Universal Programmer. In some cases a home-built programmer and potentiostat/galvanostat combination were used. Data were recorded on either a Soltec Model VP-6423S, Hewlett Packard Model 7045B X-Y recorder, or a Nicolet 4094 Digital Oscilloscope. The oscilloscope was used to transfer capacitance and photocurrent data to an IBM AT personal computer, and the LOTUS 123 program was used for data analysis. Capacitance measurements were carried out by using a Princeton Applied Research Model 5204 lock-in analyzer in conjunction with a Hewlett Packard Model 200CDR oscillator which provided a sinusoidal signal of 10 mV (peak to peak).

Irradiation of the electrode was performed with either a beam-expanded Spectra Physics 5 mW He/Ne laser or with an Oriel Model 6130 100-W quartz/halogen lamp. A Laser Precision Model CTX-534 light chopper and an Oriel Model 7240 monochromator were used when performing photocurrent spectral measurements. The intensity of illumination was determined by using an EG&G Electro-Optics Model 450-1 radiometer/photometer.

Scanning electron micrographs (SEM) and semiquantitative x-ray fluorescence analysis were performed on a Jeol Model JSM35C or a Jeol 733 Super Probe scanning electron microscope equipped with energy and wavelength dispersive spectrometers.

(c) Solvents and electrolytes.—Experiments were performed either in acetonitrile (Burdick & Jackson distilled in glass) which was dried over 4Å molecular sieves or water which was passed through a Hydro-System purification train yielding water with resistance of at least 18 MΩ. Tetrabutylammonium perchlorate (TBAP) (G. F. Smith), which had been recrystallized three times from ethyl acetate and dried under vacuum for 72h, was used when working with acetonitrile. KBr, KCl, or Na$_2$SO$_4$, which were reagent grade and were used without further purification, were the electrolytes when using water as a solvent. All solutions were purged with N$_2$ or Ar for at least 20 min prior to experimentation. A conventional three electrode, single compartment cell (15 ml of volume) fitted with a flat optical Pyrex window for illumination was used for all experiments. A large area platinum gauze was used as a counterelectrode. All potentials are reported *vs.* the sodium saturated calomel electrode (SSCE) when working in nonaqueous solvents or *vs.* the saturated calomel electrode (SCE) when working in water.

Table I. Experimental data for the synthesis of the polycrystalline thin films

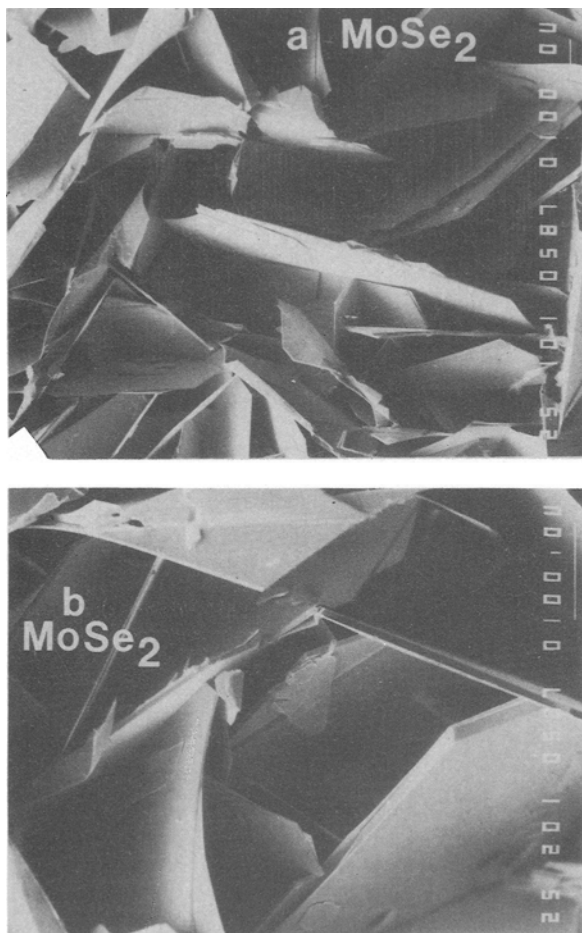| Compound	Grams	Temperature (°C)	Time (h)
WSe$_2$ Ref. (17)	10	850	72
WS$_2$	10	1040	72
MoSe$_2$ + Se^0	10 0.13	1130	7 days

Fig. 1. Scanning electron micrographs (SEM) of PTF of $MoSe_2$ prepared with added Se^0. (a) Low magnification (100×) and (b) high magnification (200×).

Fig. 2. SEM of PTF of $MoSe_2$ prepared without added Se^0. (a) Low magnification (1000×) and (b) high magnification (3200×).

Results and Discussion

(a) Synthesis and surface morphology.—The experimental conditions for the synthesis of the PTF of p-WSe_2, p-WS_2, and p-$MoSe_2$ are presented in Table I. However, the product of the synthesis of the polycrystalline thin fillms of p-WS_2 and p-$MoSe_2$ contained single crystals as well. In the synthesis of the polycrystalline thin films of p-WSe_2, single crystals could be obtained when the growth was at 1000°C for 7 days. For the synthesis of the polycrystalline thin films of $MoSe_2$, Se^0 was added as a transporting agent in order to obtain an increase in the crystallite size. Figures 1 and 2 show scanning electron micrographs of PTF of p-$MoSe_2$ with and without Se^0 added in the synthesis, respectively (note the difference in the scales). The effect of Se^0 addition was anticipated since it is known that it helps in the transport rate of the compound. On the other hand, for the synthesis of p-WSe_2 and p-WS_2, this was not required, since the crystallite sizes were quite large (Fig. 3 and 4). A puzzling result of the syntheses is that for all three compounds the products were always p-type. We attribute this to impurities in the original powder as well as to partial nonstoichiometries.

As can be seen in Fig. 1a, 3a, and 4a, the surfaces of these thin films are composed of randomly oriented plates, and under higher magnification (Fig. 1b, 3b, and 4b) the plates appear quite smooth, free of imperfections. The overall structure of the films can be described as single crystals randomly placed together. Semiquantitative analysis by x-ray fluorescence showed that the polycrystalline thin films had the expected ratio of 1:2 for transition metal to chalcogenide.

(b) Photocurrent spectra.—Photocurrent spectra of the PTF were obtained in a solution of 10 mM chloranil and 0.1M TBAP in acetonitrile, at an applied potential of +0.3V *vs.* SSCE. Figure 5 shows the photocurrent spectra of
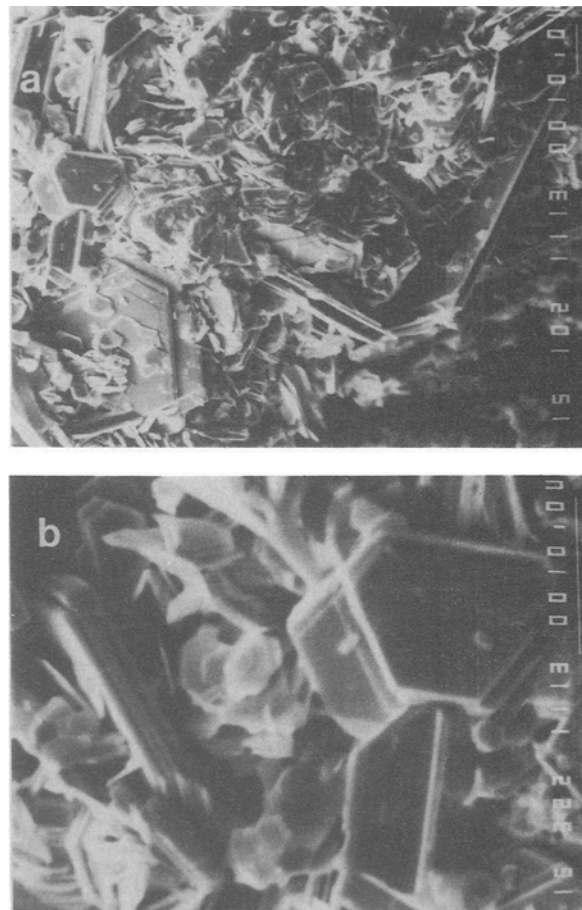
p-WSe_2, p-WS_2, and p-$MoSe_2$ films. For p-WSe_2, the quantum efficiency begins to increase at about 860 nm with a peak at 780 nm. This spectrum correlates very well with that reported by Gerischer (19) and co-workers and Kam and Parkinson (8) for single crystals, as well as with the absorption spectrum for WSe_2 (20). For p-WS_2, the QE begins to increase at 900 nm, but the increase is slow. A sharp increase is noticed at 650 nm, with a peak at 620 nm. This last peak is in the energy region of the direct transition. In addition, this spectrum is similar to the absorption spectrum presented by Beal *et al.* (20). It is however, somewhat shifted relative to that reported by Kam and Parkinson (8), although the spectral details are similar. For p-$MoSe_2$, the quantum efficiency starts to increase at approximately 900 nm with a peak at 790 nm, correlating very well with the spectrum reported by Tributsch (1) and others (8) for single-crystal $MoSe_2$. In addition, it is also similar to the absorption spectrum presented by Beal *et al.* (21).

A plot of the square of the photocurrent *vs.* light energy (eV) in the rising portion of the curve yields a straight line (see Fig. 6a) for the three PTF from which a direct bandgap energy can be extrapolated. The results are presented in Table II. All of the values obtained correlated very well with previous results reported for single crystals (see Table II).

If, on the other hand, the data are plotted as the square root of the photocurrent *vs.* light energy, a straight line (see

Table II. Direct and indirect bandgap energies of PTF of WSe_2, WS_2, and $MoSe_2$

Semiconductor	Indirect Bandgap (eV)		Direct Bandgap (eV)	
	PTF	Single crystal	PTF	Single crystal
WSe_2	1.37	1.40 (23)	1.57	1.57 (19)
WS_2	1.29	1.31 (26)	1.89	1.80 (25)
$MoSe_2$	1.26	1.10 (24)	1.47	1.38 (5)

Fig. 3. SEM of PTF of WSe$_2$. (a) Low magnification (60×) and (b) high magnification (100×).
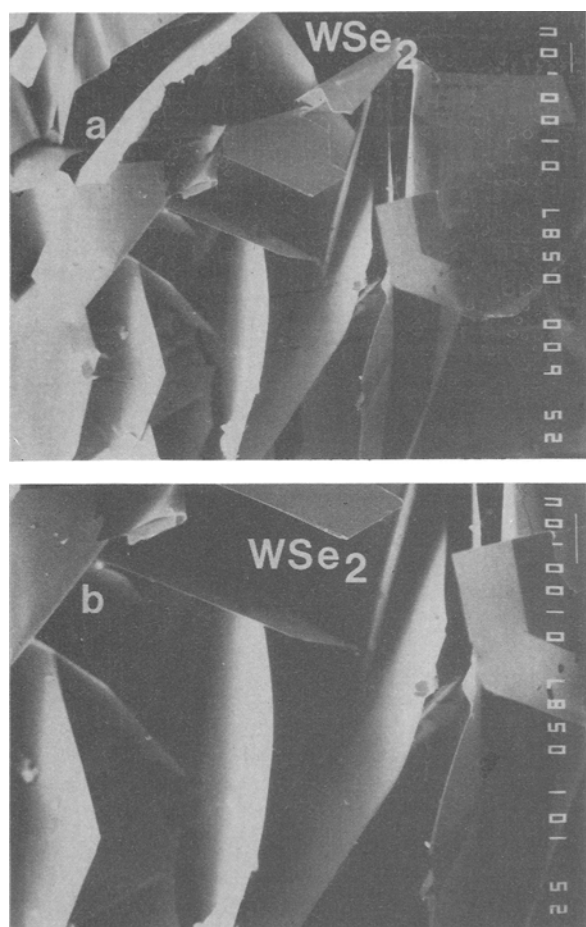

Fig. 4. SEM of PTF of WS$_2$. (a) Low magnification (200×) and (b) high magnification (400×).

Fig. 6b) is also obtained from which an indirect bandgap energy can be obtained. As expected (22), this value is smaller than the direct transition. For WS$_2$, the values obtained are quite close to those reported in the literature for single crystals (see Table II). However, for WSe$_2$ and MoSe$_2$, they are somewhat higher than reported values (23-26). Nonetheless, these results indicate that the polycrystallinity of these materials does not significantly alter the nature of the optical transitions.

(c) Differential capacitance measurements.—In order to ascertain the energetic location of the Fermi level of the PTF, differential capacitance measurements were performed. From a plot of $1/C^2$ *vs.* E (applied potential *vs.* SCE) one can determine the flatband potential and the ac-
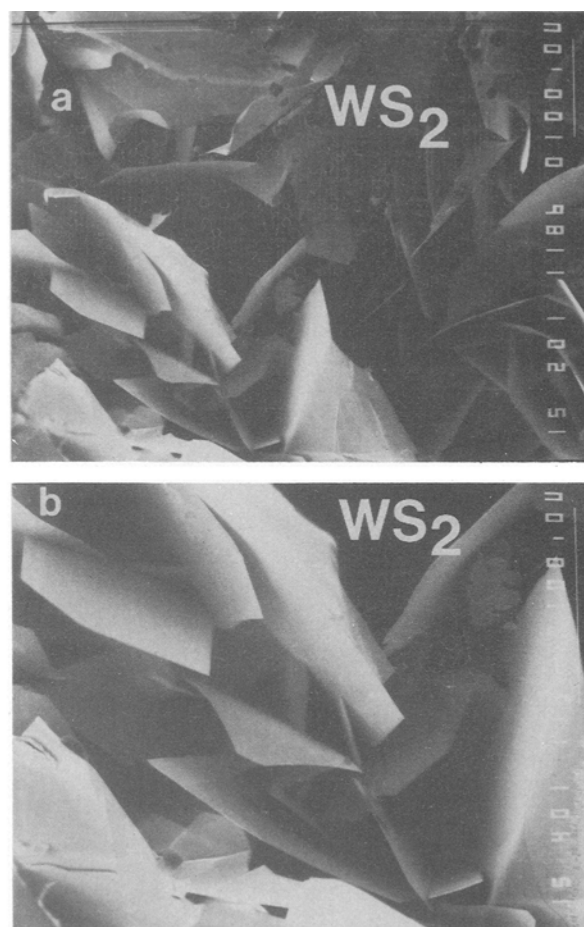
ceptor density (N_A) from the intercept and the slope, respectively. The experiments were performed in the dark in a solution of 0.2M Na$_2$SO$_4$ at different pH (4, 7, 9.7). The values of the flatband potentials as well as the acceptor densities are presented in Table III. For the three PTF, the flatband (E_{FB}) potential varied with pH, with the trend being a more negative FB with increasing pH (see Fig. 7). This was anticipated due to the high density of exposed edges in the PTF where OH$^-$ ions can adsorb and shift the Fermi energy to more negative value. The largest shift was at a pH of 9.7. At this pH, the FB was shifted 200-300 mV negative relative to the value at pH 7. On the other hand, at pH 4 the difference with respect to pH 7 was much smaller indicating that the surface adsorption sites are relatively basic. However, the flatband potentials, at pH 7, for WSe$_2$ and

Table III. Flatband potentials (E_{FB}), acceptor densities (N_A), and valence band potentials (E_V) for the PTF semiconductors

PTF semiconductors	E_{FB} *vs.* SCE			N_A (cm^{-3})	E_V (E *vs.* SCE)
	pH 4.0	7	9.7		
p-WSe$_2$	0.78 ± 0.06	0.75 ± 0.06	0.53 ± 0.06	5 × 10^{17} 2	0.80
p-MoSe$_2$	0.85 ± 0.07	0.74 ± 0.05	0.60 ± 0.03	4 × 10^{18} 2	0.84
p-WS$_2$	1.2 ± 0.1	0.9 ± 0.1	0.6 ± 0.1	7 × 10^{17} 3	1.1

Table IV. V_{oc} for the PTF semiconductors in different redox systems. Irradiation was provided with a He/Ne laser at 12 mW/cm^2

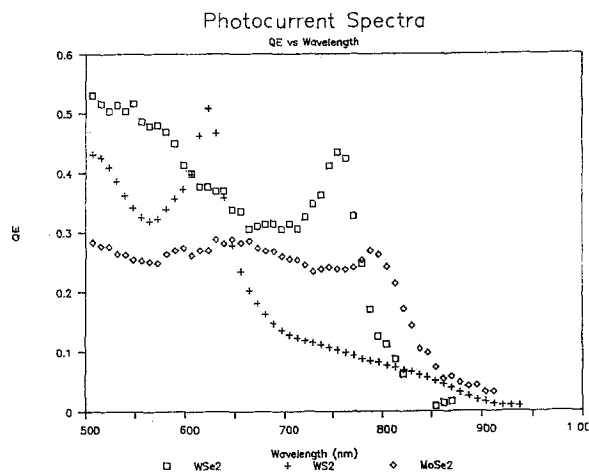|		V_{oc} (mV)		
Redox couple	$E_{1/2}$[a]	WS$_2$	WSe$_2$	MoSe$_2$
Fe(CN)$_6^{-3/-4}$	+0.45	380	160	240
Ferrocene$^{+/0}$	+0.43	140	30	10
TCNQ	+0.21	380	70	110
Co(bpy)$_3^{+3/+2}$	+0.05	520	200	200
Chloranil	+0.05	540	300	300
MV$^{+2/+1}$	-0.41	270	60	70

[a] *vs.* SSCE

Fig. 5. Photocurrent spectra of PTF of p-WSe$_2$, p-WS$_2$, and p-MoSe$_2$ in 10 mM chloranil in acetonitrile containing 0.1M TBAP and at an applied potential of +0.3V *vs.* SSCE.

Fig. 7. Plot of flatband potentials of the PTF of p-WSe$_2$, p-WS$_2$, and p-MoSe$_2$ *vs.* pH.

WS$_2$ correlate very well with those reported in the literature for single crystals (0.72 *vs.* SCE for p-WSe$_2$ (26) and 0.95 *vs.* SCE for p-WS$_2$ (25)). When performing the capacitance measurements, it was found that the intercept as well as the slope of the Mott-Schottky plot were relatively constant for frequencies in the range of 700-1500 Hz. However, if the frequency was higher than 1500 Hz, the FB potential as well as the slope showed some dispersion. This deviation at high frequencies can be explained in terms of a high density of surface states in the PTF (27).
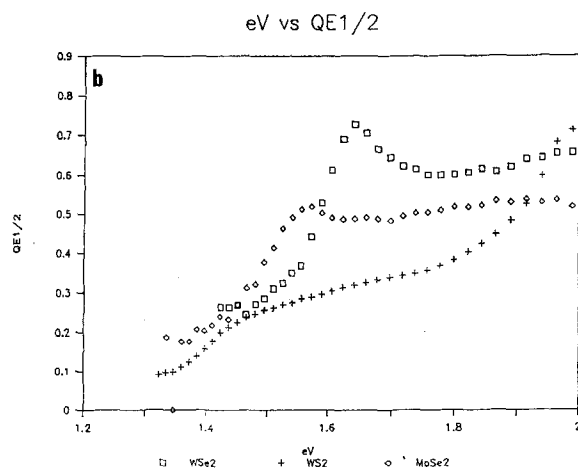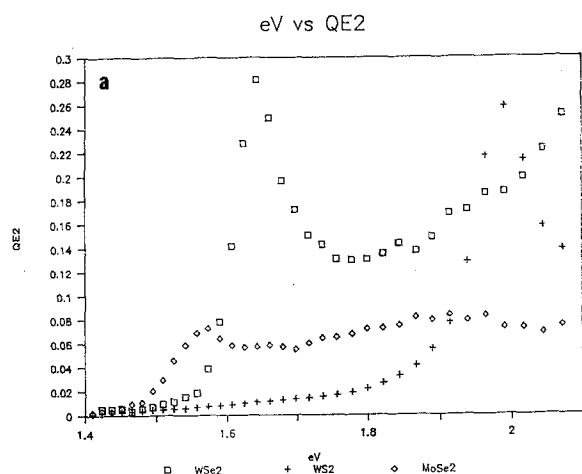

Fig. 8. Schematic representation of the energetic location of the conduction and valence bands of the PTF of p-WSe$_2$, p-WS$_2$, and MoSe$_2$ with respect to the SCE and the redox systems used.

Fig. 6. (a) Plot of the square of the quantum efficiency (QE^2) *vs.* light energy (eV) (direct bandgap determination) and a plot of (b) QE$^{1/2}$ *vs.* eV for the determination of the indirect transition of the PTF of p-WS$_2$, p-WSe$_2$, and p-MoSe$_2$.
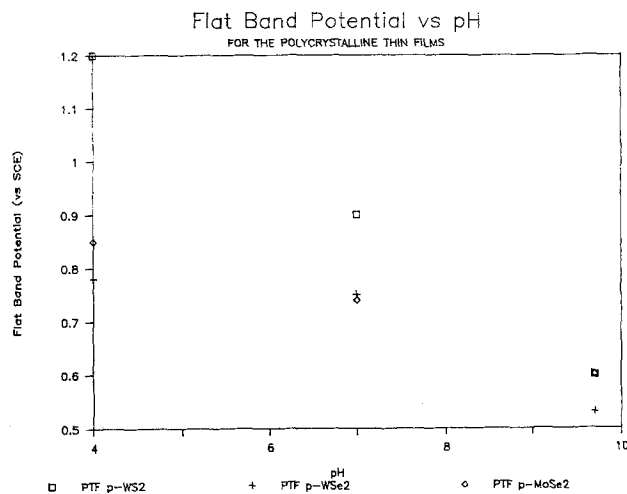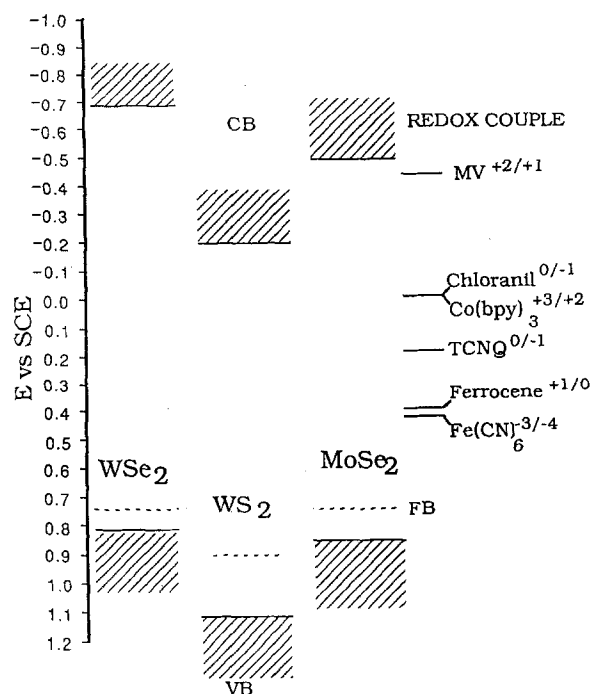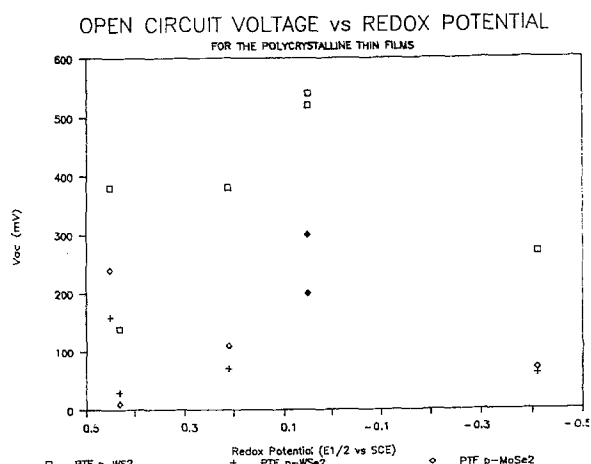

Fig. 9. Plot of V_{oc} *vs.* E_{redox} for the PTF of p-WSe$_2$, p-WS$_2$, and MoSe$_2$ under illumination with a He/Ne laser (632.8 nm, 12 mW/cm^2).
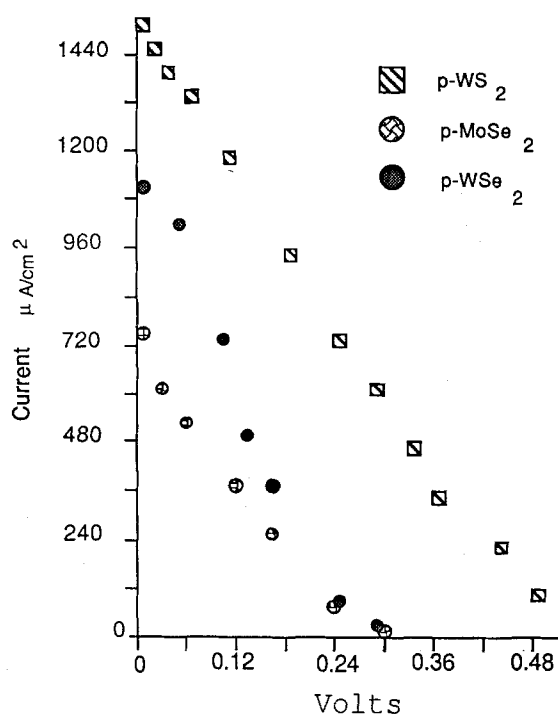
Fig. 10. Current-voltage curves for the PTF of p-WSe₂, p-WS₂, and MoSe₂ in chloranil⁰/⁻¹ 10 mM/1 mM.

Fig. 12. Current-voltage curves for the PTF of p-WSe₂, p-WS₂, and MoSe₂ in $Fe(CN)_6^{-3/-4}$ (0.05M/0.005M).

The N_A values calculated from the slopes were rather high. However, one has to consider the fact that we measure the geometric area and not the real surface area, and for these materials this represents a very large deviation. A more realistic value of N_A would be one that is 1-2 orders of magnitude smaller. Using the acceptor density and the FB potential, one can locate the valence band by using the following equation (28)

$$N_A = N_V e^{-(E_F - E_V)/kT}$$

where N_V is the density of states in the valence band which can be calculated with the following expression (28)
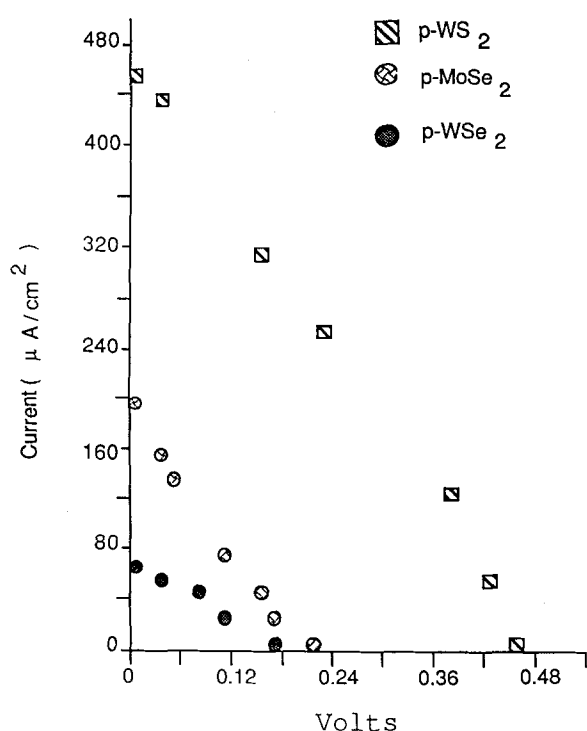
$$N_V = 2(2pm_p kT/h^2)^{3/2}$$

where m_p is the effective mass of the hole (h⁺). In our calculations we will assume that $m_p = m_o$ (29), where m_o is the mass of a free electron. In addition we will assume that the effective mass of the hole (h⁺) is equal for the three polycrystalline thin films. Making these approximations we can obtain a value for $N_V = 2.5 \times 10^{19}$ cm⁻³. Therefore, the E_V values for WSe₂, WS₂, and MoSe₂ are 0.8, 1.1, and 0.84V vs. SCE, respectively (see Table III). Taking these values along with the bandgap energies determined, we can construct energy level diagrams for the polycrystalline semiconductors, and these are shown in Fig. 8.

(d) Photovoltaic cells and cyclic voltammetry.—Open-circuit voltages (V_{oc}) and short-circuit currents (I_{sc}) for the polycrystalline thin films, in different redox systems, were measured by using a He/Ne laser (632.8 nm, 12 mW/cm²) as the light source. Table IV lists the V_{oc} values measured for the PTF in the different redox systems, and it can be seen that p-WS₂ had the highest V_{oc} (0.5V) and I_{sc} (1.5 mA/cm²). Figure 9 shows a plot of V_{oc} vs. $E_{1/2}$. The slope of the plot of

Fig. 11. Current voltage curves for the PTF of p-WSe₂, p-WS₂, and MoSe₂ in Co(bpy)₃⁺³/⁺² (10 mM/1 mM).
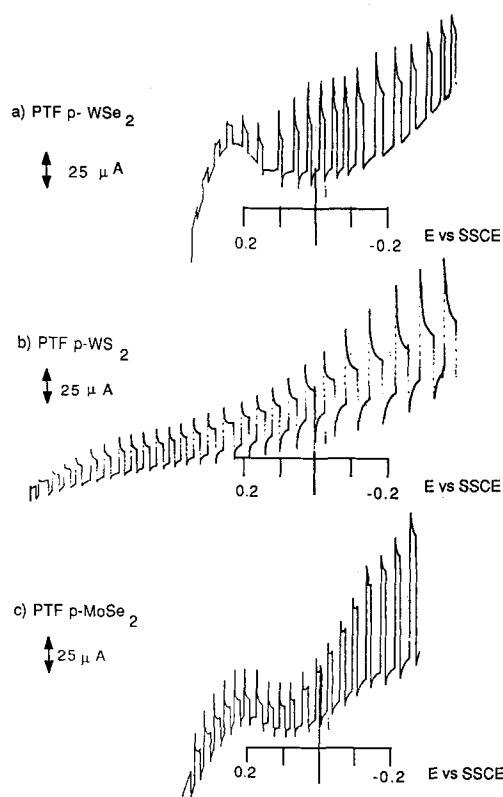

Fig. 13. Cyclic voltammetry of (a) PTF p-WSe₂, (b) PTF p-WS₂, and (c) PTF p-MoSe₂ in 10 mM MV⁺⁺ and 0.1M TBAP under chopped illumination.

Table V. Open-circuit voltages (V_{oc})^a, short-circuit currents (I_{sc}),^{b} fill factors (FF), and efficiencies (η)^c for the polycrystalline thin film (PTF) semiconductors (SC) in redox couples A, B, and C.

A = Chloranil^0 10 mM, chloranil^{-1} 1 mM, and 0.1M TBAP in acetonitrile
B = Co(bpy)$_3^{+3}$ 10 mM, Co(bpy)$_3^{+2}$, and 0.1M KCl in water
C = Fe(CN)$_6^{-3}$ 0.05M, Fe(CN)$_6^{-4}$ 0.005M, and 0.1M KCl in water

PTF SC	Redox couple A				Redox couple B			
	I_{sc}	V_{oc}	FF	$\eta\%$	I_{sc}	V_{oc}	FF	$\eta\%$
p-WSe$_2$	1.1	300	0.22	0.6	0.06	195	0.23	0.02
p-WS$_2$	1.5	540	0.22	1.5	0.40	520	0.26	0.5
p-MoSe$_2$	0.75	300	0.20	0.4	0.20	210	0.20	0.07

PTF SC	Redox Couple C			
	I_{sc}	V_{oc}	FF	$\eta\%$
p-WSe$_2$	0.65	160	0.27	0.2
p-WS$_2$	1.50	380	0.39	1.9
p-MoSe$_2$	0.75	240	0.28	0.4

^{a} V_{oc} in mV
^{b} I_{sc} in mA/cm^2
^{c} Irradiation with a He/Ne laser (12 mW/cm^2)

V_{oc} vs. E_{redox} for p-WS$_2$ is approximately 1, close to the value for an ideal semiconductor. For the other PTF semiconductors, however, the slope is much smaller. Photocurrent-voltage measurements were obtained in three different redox systems which gave the highest V_{oc}. These systems were (A) chloranil^0 10 mM, chloranil^{-1} 1 mM, and 0.1 TBAP in acetonitrile; (B) Co(bpy)$_3^{+3}$ 10 mM, Co(bpy)$_3^{+2}$ 1 mM, and 0.1M KCl in water; (C) Fe(CN)$_6^{-3}$ 0.05M, Fe(CN)$_6^{-4}$ 0.005M, and 0.1M KCl in water.

The I-V curves obtained when using these three systems are shown in Fig. 10, 11, and 12, respectively. In system A the highest efficiency (η) was for the PTF of p-WS$_2$, giving a value of 1.5%, whereas p-MoSe$_2$ and WSe$_2$ gave values of 0.4 and 0.6%, respectively (see Table V). For system B the efficiencies were lower for all three PTF. For system C, the highest efficiencies were obtained with p-WS$_2$ having the highest at about 1.9%.

When performing cyclic voltammetry with chopped illumination in 5 mM methyl viologen in acetonitrile containing 0.1M TBAP, it was found that the PTF of p-WSe$_2$ (Fig. 13a) and p-MoSe$_2$ (Fig. 13c) had a higher dark current at positive potentials when compared to the PTF of p-WS$_2$ (Fig. 13b). We believe that this can be due to metallic Se^0 being oxidized on the edges, since, in a previous study on p-WSe$_2$ we found that the surface was enriched in selenium (30). This may explain why the efficiencies of PTF of MoSe$_2$ and WSe$_2$ were smaller when compared to WS$_2$.

Conclusions

We have prepared and characterized polycrystalline thin films of p-WSe$_2$, p-WS$_2$, and p-MoSe$_2$ which exhibit reasonable photoelectrochemical behavior. The PTF of p-WS$_2$ exhibited the best characteristics in terms of open-circuit voltages and short-circuit currents. We attribute this to surface impurities; especially Se^0, which is present in the films of WSe$_2$ and MoSe$_2$ but not in WS$_2$. We have also characterized the band structures for all of the films, and the values we obtain correlate well with those published for single crystals. Although at this time the overall conversion efficiencies are modest, we believe that further modification of the surface of these materials should result in enhanced photoelectrochemical characteristics.

Acknowledgments

REFERENCES

1. E. Becquerel, *C. R. Acad. Sci.*, **9**, 561 (1839).
2. W. H. Brattain and G. G. B. Garett, *Bell Syst. Tech. J.*, **34**, 129 (1955).
3. (a) A. Fujishima, K. Honda, and S. Kikuchi, *J. Chem. Soc. Jpn.*, **72**, 108 (1969); (b) A. Fujishima and K. Honda, *Nature (London)*, **37**, 2381 (1972).
4. A. J. Nozik, *Ann. Rev. Phys. Chem.*, **29**, 189 (1978).
5. (a) H. Tributsch, *Ber. Bunsenges. Phys. Chem.*, **81**, 361 (1977); (b) *ibid.*, **82**, 189 (1978).
6. (a) H. Tributsch and J. S. Bennet, *J. Electroanal. Chem.*, **81**, 97 (1977); (b) H. Tributsch, *This Journal*, **125**, 1086 (1978).
7. (a) W. Kautek, H. Gerischer, and H. Tributsch, *Ber. Bunsenges. Phys. Chem.*, **83**, 1000 (1979); (b) H. J. Lewerenz, H. Gerischer, and M. Lubke, *This Journal*, **131**, 100 (1984).
8. K. K. Kam and B. A. Parkinson, *J. Phys. Chem.*, **86**, 463 (1982).
9. (a) H. S. White, F-R. Fan, and A. J. Bard, *This Journal*, **128**, 1045 (1981); (b) D. Canfield and B. A. Parkinson, *J. Am. Chem. Soc.*, **103**, 1279 (1981).
10. Extensive work has been done to improve the crystallite size, but without much success. For example, see (a) A. A. Al-Hilli and B. L. Evans, *J. Cryst. Growth*, **15**, 93 (1972); (b) M. K. Agarwal, H. B. Patel, and K. Nagiredy, *ibid.*, **41**, 84 (1977); (c) M. K. Agarwal, P. D. Patel, J. V. Patel, and J. D. Kshatriya, *Bull. Mat. Sci.*, **6**, 549 (1984).
11. H. J. Lewerenz, A. Heller, and F. J. DiSalvo, *J. Am. Chem. Soc.*, **102**, 1877 (1980).
12. (a) D. C. Bookbinder and M. S. Wrighton, *ibid.*, **102**, 5123 (1980); (b) D. C. Bookbinder, N. S. Lewis, M. G. Bradley, A. B. Bocarsly, and M. S. Wrighton, *ibid.*, **101**, 7721 (1979); (c) D. C. Bookbinder, J. A. Bruce, R. N. Dominey, N. S. Lewis, and M. S. Wrighton, *Proc. Nat. Acad. U.S.A.*, **77**, 6280 (1980).
13. (a) R. J. Nelson, J. S. Williams, H. J. Leamy, B. Miller, H. C. Casey, Jr., B. A. Parkinson, and A. Heller, *Appl. Phys. Lett.*, **36**, 76 (1980); (b) W. D. Johnston, Jr., H. J. Leamy, B. A. Parkinson, A. Heller, and B. J. Miller, *This Journal*, **127**, 90 (1980).
14. G. Kline, K. Kam, R. Kiegler, and B. A. Parkinson, *Solar Energy Mat.*, **6**, 337 (1982).
15. G. Kline, K. Kam, D. Canfield, and B. A. Parkinson, *ibid.*, **4**, 301 (1981).
16. (a) G. Djemal, N. Muller, U. Lachish, and D. Cahen, *ibid.*, **5**, 403 (1981); (b) D. S. Ginley, R. M. Biefeld, B. A. Parkinson, and K. K. Kam, *This Journal*, **129**, 145 (1982); (c) L. F. Schneemeyer and U. Cohen, *ibid.*, **130**, 1536 (1983); (d) A. Di Paola, *Mater. Res. Bull.*, **22**, 569 (1987).
17. C. R. Cabrera and H. D. Abruña, *J. Phys. Chem.*, **89**, 1279 (1985).
18. C. R. Cabrera and H. D. Abruña, *J. Electroanal. Chem.*, **206**, 101 (1986).
19. J. Gobrecht and H. Gerischer, and H. Tributsch, *Ber. Bunsenges. Phys. Chem.*, **82**, 1331 (1978).
20. A. R. Beal, W. Y. Liang, and H. P. Hughes, *J. Phys. C.*, **9**, 2449 (1976).
21. A. R. Beal and H. P. Hughes, *ibid.*, **12**, 881 (1979).
22. C. Kittel, "Introduction to Solid-State Physics," John Wiley and Sons, New York (1976).
23. C. J. Lewerenz, S. D. Ferris, C. J. Doherty, and H. J. Leamy, *This Journal*, **129**, 418 (1982).
24. J. A. Baglio, G. S. Calabrese, E. Kamieniecki, R. Kershaw, C. P. Kubiak, A. J. Ricco, A. Wold, M. S. Wrighton, and G. D. Zoski, *ibid.*, **129**, 1461 (1982).
25. J. A. Baglio, G. S. Calabrese, D. J. Harrison, E. Kamieniecki, A. J. Ricco, M. S. Wrighton, and G. D. Zoski, *J. Am. Chem. Soc.*, **105**, 2246 (1983).
26. F-R. Fan and A. J. Bard, *This Journal*, **128**, 945 (1981).
27. V. A. Myamlin and Y. V. Pleskov, "Electrochemistry of Semiconductors," chap. 3, Plenum Press, New York (1966).
28. S. R. Morrison, "Electrochemistry at Semiconductors and Oxidized Metal Electrodes," Plenum Press, New York (1980).
29. W. T. Hicks, *This Journal*, **111**, 1058 (1964).
30. C. R. Cabrera, H. D. Abruña, S. Simko, and R. W. Murray, *Sol. Energy Mat.*, **15**, 277 (1987).